RSC Advances

ROYAL SOCIETY OF CHEMISTRY

www.rsc.org/advances

A DFT-D study on the interaction between lactic acid and single-wall carbon nanotubes

Alireza Najafi Chermahini*[a], Abbas Teimouri [b], Hossein Farrokhpour [a]

[a] *Department of Chemistry, Isfahan University of Technology, 84154-83111 Isfahan, Iran, e-mail: anajafi@cc.iut.ac.ir or najafy@gmail.com*

[b] *Chemistry Department, Payame Noor University (PNU), Tehran 19395-4697, Iran*

Abstract

Density functional theory (DFT) was used to investigate the adsorption of lactic acid (LA) molecule on the surface of (4,4), (5,5), (6,6) and (7,7) single-walled carbon nanotubes (SWCNTs). A hybrid DFT method with the inclusion of dispersion correction was employed and the results compared to those obtained from the non-corrected DFT method. The energies and optimum distances for two different configurations were obtained after relaxation of the entire system. The calculations showed that the adsorption of lactic acid onto outer wall of carbon nanotubes was thermodynamically favored. The adsorption of lactic acid outside the CNT with (4,4) chirality and via a vertical orientation to the tube axis above the center of a hexagon surface and through its hydroxyl group was the most stable state of physisorption with the adsorption energy of -13.39 kcal/mol. Total density of states (TDOS) and projected density of states (PDOS) analysis in the vicinity of Fermi level region suggested that the electronic states to be contributed from SWCNT rather than lactic acid. The DFT calculations also showed that non-covalent functionalization of SWCNTs with lactic acid could give rise to new impurity states in the DOS of pristine CNTs and suggested possible carrier doping of carbon nanotubes via selective adsorption of molecule. The global reactivity descriptors in the gas phase and solvent calculated.

1. Introduction

Since the last two decades, carbon nanotubes (CNTs) have attracted enormous practical and scientific attention due to their physical, optical, electronic, magnetic, and thermodynamic properties with potential applications in nanoelectronics, energy storage, chemical processes, biosensors, field emission displays and medical diagnostics and therapy. [1-11] It has been pointed out that the electronic properties of CNTs can be moderated by vacancy defects, [12, 13] electronic field, [14] filling some species inside the CNTs [15-17] and physical or chemical adsorptions on the side wall of the tubes. [18-22] In the other hands, non-covalent modification of CNTs has been developed for various types of applications such as drug delivery, biochemical sensors, gene delivery and therapeutic applications. [23-26]

Lactic acid (LA) or 2-hydroxypropanoic acid is a chiral organic acid of biological significance. [27, 28] The biological importance of lactic acid is mainly due to its function as metabolite. LA is the main final product of lactic acid bacteria (LAB) metabolism. In addition, it is made in eukaryotic cells, after glucose anaerobic metabolism. [29] In the other hands, LA has particularly interested for its use in producing biodegradable LA polymers, solvents, metal pickling and food additives. [30-32] Because of its widespread influence, LA has been subjected of many theoretical and experimental studies. Conformational analysis of LA using microwave spectroscopy studied by van Eijck in the gas phase and it was found that an intramolecular hydrogen bond from the proton of hydroxyl group to the carbonyl oxygen atom is formed. [33] The van Eijck results were also confirmed by Borba *et. al.* through the study of conformational analysis of LA by matrix-isolation FT-IR spectroscopy and theoretical calculations. [34] Schouten *et. al.* determined the structure of LA at 100 K and found that carboxylic group at the side of the carbonyl oxygen atom is almost planar with the oxygen atom of aliphatic hydroxyl group. [35]

Cassanas and co-workers, using IR and Raman spectroscopy, showed that LA forms dimers via intermolecular association compounds connected by hydrogen bonds in the aqueous solution. [36] Protonation of LA was studied in the gas phase by Berruyer-Penaud and his co-workers and they showed that the protonation of LA leads to decomposition and CO losing. [37] Pecul *et al.* studied conformers of LA , theoretically, at the HF and MP2 levels of theory and found only two stable conformers . [38] In a recent study, Smaga and Sadlej calculated the energy and geometrical parameters of 1:1 and 1:2 chiral LA:water complexes at the MP2/aug-cc-pVDZ level of theory and found that the stabilization of complexes dominated by exchange and induction effects. [39]

Determination of LA is critical in food industry, clinical diagnosis and sports medicine. Its determination in medicine is useful for monitoring respiratory insufficiency, shocks, heart failure and metabolic disorders. In this paper, our aim is the evaluation of the ability of SWCNTs as a candidate for the detection of LA in the gas phase and aqueous medium. For this propose, the most stable conformation of LA, where there is an internal hydrogen bond between proton of hydroxyl group and oxygen of carbonyl group of carboxylic acid moiety, is considered. In continuum with our previous studies on the interaction of biologically important molecules with nanotubes, [40, 41] our aim is the investigation of the non-covalent functionalization of pristine (4,4) (5,5), (6,6) and (7,7) SWCNTs with lactic acid molecule.

2. Computational details

A SWCNT is classified into three types, namely, armchair nanotubes (n, n), zigzag nanotubes (n, 0), and chiral nanotubes (n, m) with n≠m. In this paper, the armchair CNTs with (4,4), (5,5),

(6,6), and (7,7) chiralities were selected. All calculations were performed on the DMol3 module of Materials Studio. [42, 43] The generalized gradient approximation (GGA) method proposed by Perdew and Wang (PW91) was used to deal with the exchange and correlation functional. [44] All-electron Kohn–Sham wave functions are expanded in a double numerical basis with polarized orbital (DNP), in which the 2s and 2p orbital are used for carbon. The (DNP) function, equivalent to 6–31 G (d,p) basis set of Gaussian basis set. It is well known that LDA cannot explain properly the dispersion forces between molecules, which severely act in the limit of negligible overlap between electron densities. Therefore, the LDA function tends to overestimate the interaction energy between two molecules. The GGA corrects these errors, and GGA functional provides a better overall description of the electronic subsystem than the LDA functional. [45] The energy tolerance accuracy, maximum force, and displacement were set as 10^{-5} Ha, 2×10^{-3} Ha/Å, and 5×10^{-3} Å, respectively. In order to accurately describe the van der Waals (vdW) interaction, the dispersion-corrected DFT (DFT-D) scheme put forward by Ortmann, Bechstedt, and Schmidt (OBS) [46] was used. Solvation calculations on pristine nanotube and CNTs/LA complexes were performed with the aid of conductor like screening model (COSMO) as implemented in DMol3 program at the LDA/DNP (fine) level of theory. [47-49]

The quantum molecular descriptors for nanotubes were determined as follows:

$$\mu = -\chi = -\frac{1}{2}(I + A)$$

$$\eta = \frac{1}{2}(I - A)$$

$$\omega = \frac{\mu^2}{2\eta}$$

where I ($-E_{HOMO}$) is the energy of the Fermi level and A ($-E_{LUMO}$) is the first given value of the conduction band. The electronegativity (χ) is determined as the negative of chemical potential (μ), as follows: $\chi = -\mu$. In addition, hardness (η) can be approximated using the Koopmans' theorem.

The effect of solvent was modeled by the conductor-like screening model (COSMO), [50] where water has been used as solvents. COSMO is a considerable simplification of the continuum solvation model (CSM) without significant loss of accuracy. [51] For solvation studies, water which has the highest dielectric constant (78.4) is taken as solvating media as it mimics human biological system to recognize the behavior of CNT/LA complexes in the body. In the continuum solvation models such as COSMO, solvation occurs by insertion of the solute in a cavity which bounded by a dielectric continuum. The charge distribution of the solute polarizes the dielectric medium which is described by the generation of screening charges in the cavity. Unlike other continuum models, COSMO allows geometry optimization within the continuum and thus gives a good description of the electrostatic interactions at the cavity. The free energy of solvation is defined as the free energy of transfer of one mole of solute from an ideal gas state to an infinitely dilute solution. This free energy is calculated by Dmol3 software based on the following formula:

$$\Delta G_{Solv} = (E + \Delta G_{nonelectrostatic}) - E^{\circ} \qquad (1)$$

where E° is the total DMol energy of the molecule in gas phase, E is the total DMol/COSMO energy of molecule in the solvent, and $\Delta G_{nonelectrostatic}$ is the nonelectrostatic due to dispersion and cavity formation effect.

DMol3 uses numerical functions on an atom centered grid as its atomic basis. These basis sets were constructed specifically for use in DFT calculations. Their high quality minimizes or even removes basis set superposition error (BSSE) effects. [52, 53] Inada and Orita by using the numerical basis sets like DNP have shown that the BSSE for the binding energies are very small. Therefore, in the present study the interaction energies were calculated without the correction of BSSE. [54]

For accurately comparing the energies, GGA/TNP (triple numeric with polarization) single-point energies were performed on the structure optimized with DNP.

3. Results and discussion

3.1. Structures

The structures of the of SWCNTs (n, n) n=4–7 armchairs were optimized in the gas phase. The structures were allowed to relax until the forces were smaller than 0.002 Ha/Å at DFT-D/GGA level of theory. The calculated C–C bond lengths for (4, 4), (5, 5), (6, 6), and (7, 7) armchair CNTs were 1.432, 1.430, 1.429 and 1.426 Å, respectively which were in good agreement with previously reported values. [55, 56] The calculated diameters of pristine SWCNTs were 5.600, 6.948, 8.367, and 9.747 Å, respectively. The corresponding calculated diameter values agrees well with previously reported values of 5.386, 6.732, 8.079, 9.425 Å for (4, 4), (5,5), (6, 6) and (7, 7) CNTs, respectively. [57] (See Table 1).

The LA molecule was placed on the outer wall of CNTs and the system was allowed to relax with respect to all degrees of freedom without additional constraints. For the study of

adsorption, LA molecule was placed on the top of the proper CNT (over on C atom) at a distance of 2.5 Å.

Table 1
Diameters and optimum distances of nanotubes in different chiralities after optimization at DFT-D/GGA Level of theory

	CNT diameter			Optimum distance	
	pure	nnLA1	nnLA2	nnLA1	nnLA2
Gas phase					
(4,4)	5.600	5.598	5.594	2.380	2.342
(5,5)	6.948	6.937	6.941	2.262	2.941
(6,6)	8.367	8.264	8.378	2.186	2.916
(7,7)	9.747	9.742	9.737	2.483	2.907
Water					
(4,4)	5.585	5.587	5.590	2.519	2.294
(5,5)	6.942	6.956	6.934	2.213	2.942
(6,6)	8.346	8.344	8.368	2.200	2.914
(7,7)	9.744	9.725	9.739	2.219	2.499

All geometrical parameters are in Å

Two different modes were considered for the interaction of LA with CNT including adsorption through carboxylic (mode 1: LA1) and hydroxyl (mode 2: LA2) groups. The results indicated that the adsorption of target molecule can alter the diameter of nanotube. Table 1 shows that after adsorption of LA through carboxylic acid or hydroxyl group, the diameter of CNTs decreased (except adsorption of LA on CNT with (6,6) chirality via hydroxyl group). For example, adsorption of LA via its COOH functional group decreased the diameter of CNTs with (4,4), (5,5), (6,6), (7,7) chiralities to 5.598, 6.937, 8.264, and 9.725 Å, respectively. The optimum distances of LA after optimization on exterior surface of each SWCNT in two possible modes have been presented in Table 1 and Fig. 1. The shortest distance was observed when LA adsorbed on CNT with (6, 6) chirality through mode 1 (2.186 Å). The effect of solvent on the diameter of pristine CNTs is interesting. With going from gas phase to water, a regular decrease

in diameter of CNTs was observed. For example for the CNTs with (4,4) and (7,7) chirality, the diameters values decreased from 5.600 and 9.747 to 5.585 and 9.744 Å, respectively.

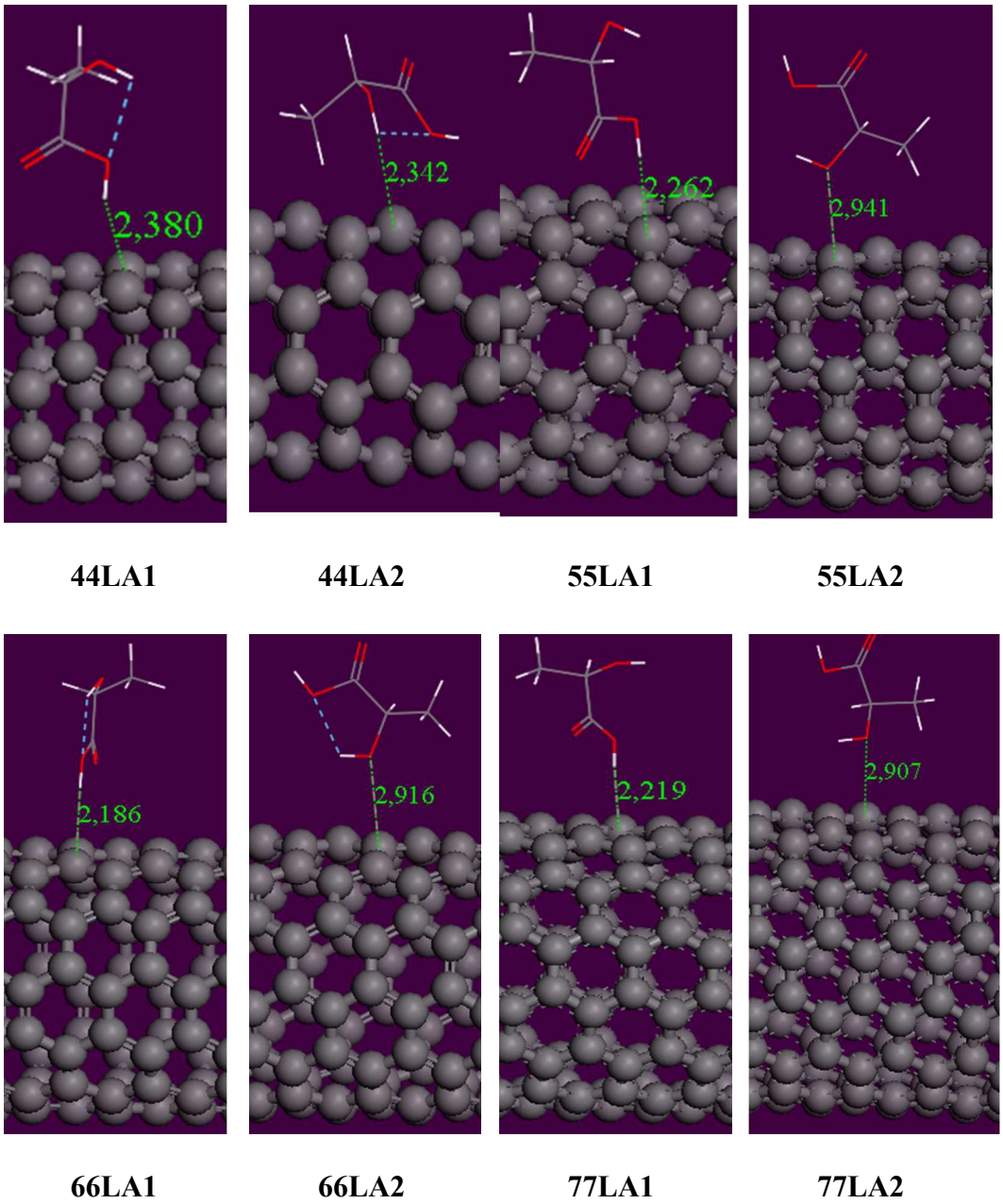

Fig.1. The optimized structures of complexes of armchair SWCNTs with LA molecule in the gas phase

A closer look at the Table 1 indicates water as a solvent has considerable effect on geometrical parameters such as optimum distances. For example, while in the gas phase lactic acid oriented via its carboxylic group in an optimum distance of 2.262 and 2.483 Å from CNT with (5,5) and (7,7) chirality, its distance shortened to 2.213 and 2.219 Å due to solvent effect.

3. 2. Adsorption and solvation energies

One of the important applications of chemical functionalization of nanotubes by various groups is to modify their electronic structures, and thus widen their potential applications. In this section, the interaction energies of LA on the exterior surface of each SWCNT in two possibilities are investigated. The adsorption energy (E_{ads}), indicating the intensity of interaction between the LA and each carbon nanotube surface, is derived according to the following equation:

$$E_{ads} = E_{CNT-LA} - E_{LA} - E_{CNT} \quad (3)$$

where E_{LA-CNT}, E_{LA}, and E_{CNT} represent the total energy of the system, the energy of the lactic acid molecule, and the energy of the corresponding SWCNT, respectively. A negative adsorption energy value corresponds to stable adsorption. In addition, the more negative is the more stable the adsorbed structure is. Table 2 represents adsorption energies of eight cases of interaction of LA and SWCNTs which calculated at DFT and DFT-D levels of theory. It should be mentioned that the calculated values of the interaction energies obtained using the DFT-D method in this work should be higher than the corresponding ab initio, although ab initio calculations has not performed in our work. For this purpose, the readers are referred to Table XX of ref. 46 that the interaction energy between two benzene molecules has been calculated using DFT-D method (GGA+vdW) and compared with the other DFT methods and ab initio methods.

A closer look at the Table 2 indicates all results are negative, which indicates that LA molecule adsorption on CNTs is energetically favored in all cases. The adsorption energy of LA on SWCNT with (4,4) chirality calculated at the DFT-D/GGA level of theory is the most negative value (-13.39 kcal/mol), which reveals that the most stable system is gained when LA through hydroxyl group approach the CNT outer surface. In addition, the adsorption of LA via carboxylic acid functional group to CNT with (4,4) chirality is strong with -8.96 kcal/mol interaction energy. The second important interaction observed for the adsorption of LA on SWCNT with (6,6) chirality with -9.76 kcal/mol, where LA approach via its carboxylic acid group to CNT surface.

Table 2
Calculated adsorption and gap energies of two configurations of lactic acid molecule on various armchair (n,n) single walled carbon nanotubes

System	E_{ad} (DFT-D)[a]	E_{ad} (DFT-D)[b]	$E_{g\ (HOMO-LUMO)}$[b]	E_{ads} (DFT)	$E_{g\ (HOMO-LUMO)}$
Gas Phase					
(4,4)	-		0.476	-	0.505
44LA1	-8.96	-6.13	0.477	-2.41	0.513
44LA2	-13.39	-10.22	0.473	-1.32	0.513
(5,5)	-		0.215	-	0.292
55LA1	-8.59	-9.80	0.220	-0.55	0.200
(55LA2	-8.08	-9.35	0.213	-1.14	0.200
(6,6)	-		0.326	-	0.316
66LA1	-8.76	-8.59	0.321	-2.38	0.313
(66LA2	-6.57	-6.79	0.323	-0.02	0.313
(7,7)	-		0.329	-	0.386
77LA1	-8.27	-9.69	0.392	-1.43	0.386
77LA2	-6.71	-7.39	0.389	-1.99	0.387
Solvent (COSMO)					
(4,4)	-		0.458	-	0.462
44LA1	-5.40	-9.88	0.458	-0.66	0.466
44LA2	-11.13	-17.22	0.455	-0.88	0.455
(5,5)			0.225	-	0.213
55LA1	-5.45	-9.36	0.238	-1.12	0.203
(55LA2	-6.39	-10.23	0.323	-0.69	0.211
(6,6)	-		0.330	-	0.422
66LA1	-6.12	-9.09	0.334	-0.10	0.323
(66LA2	-4.84	-7.50	0.330	-0.06	0.322
(7,7)	-		0.399	-	0.394
77LA1	-5.63	-9.15	0.401	-0.57	0.394
77LA2	-4.54	-7.98	0.396	-0.19	0.395

[a] Adsorption energies in kcal/mol, [b] energy gaps in eV.

[b] Adsorption energies calculated at GGA/TNP level (single point energies)

It is notable that except for CNT with (4,4) chirality that adsorb LA more effective through its hydroxyl group, for the other CNTs interaction favor through carboxylic acid adsorption. Considering the obtained results, it can be concluded that the adsorption of LA on outer walls of CNTs is possible from the energetic point of view. Table 2 compares the dispersion corrected interaction energies obtained from DFT-D/GGA calculations with those obtained based on DFT/GGA calculations. As seen, DFT/GGA results are significantly underestimated and do not show any regular trend. This means that the DFT/GGA method implemented in Dmol3 is not appropriate for calculating the interaction energies [58, 59] but, it is a good starting point to do a subsequent relaxation including the vdW forces. For more accurate evaluation of stabilities of complexes, single-point calculations at GGA/TNP level of theory was carried out. A closer look at the Table 2 indicates the stabilities are in line with GGA/DNP results but the values are more negative.

Table 2 reports the calculated interaction energies of LA with SWCNTs in the solvent. Similar to the gas phase, the adsorption energies are negative, which indicates that LA molecule adsorption on CNTs is energetically favored but the interaction energies in comparison with the gas phase have been significantly decreased. Again, it is seen that the adsorption of LA on the surface of CNT with (4,4) chirality takes place from its hydroxyl group in water. The results suggest concluding that conduction electrons have been polarized as an effect of solvation giving rise to dispersion. For more evaluation of solvent effect on physic-chemical properties of complexes, solvation energies of pristine and modified CNTs calculated and results presented in Table 3.

Table 3
Calculated solvation energies (kcal/mol) for pristine complexes of SWCNTs with LA

	SWCNT (4,4)			SWCNT (5,5)		
	Pristine	44LA1	44LA2	Pristine	55LA1	55LA2
DFT	-17.16	-26.03	-25.05	-21.56	-28.25	-31.66
DFT-D	-17.61	-25.82	-27.02	-21.74	-31.53	-29.89
	SWCNT (4,4)			SWCNT (4,4)		
	Pristine	66LA1	66LA2	Pristine	77LA1	77LA2
DFT	-25.14	-31.93	-33.07	-29.24	-35.53	-39.81
DFT-D	-25.13	-34.36	-34.43	-29.12	-38.47	-38.47

Study of solvation of biologically important molecules gives us a generalized understanding of the solubility and dissolution of modified nanotubes in aqueous media as a proxy for the biological environment. The results indicating after modification, CNTs have a higher solubility compared to pristine ones. In addition, it was observed that with the increase of diameter of CNTs, solvation energies increased regularly.

3.3. Analysis of HOMO, LUMO and electron densities

The calculated values of HOMO-LUMO energy gaps (Eg) calculated for pristine and modified carbon nanotubes with different chirality have been presented in Table 2. Carbon nanotubes with metallic behavior are expected to have a small but finite DOS near the Fermi level and the apparent gap is related to DOS peaks at the band edges of the next one-dimensional modes. It should be noted that all the $\Delta E_{LUMO-HOMOs}$ of three systems (including CNTs, and their complexes in LA1 and LA2 modes) are below 0.5 eV. As it was known, the gap of semiconductors is higher than 3 eV.

The results indicate the conductor activity of CNTs remains while the energy gap changed slightly after adsorption of LA on outer surface of CNTs. For example, after adsorption of LA on the surface of (5,5) SWCNT through its carboxylic and hydroxyl groups, the Eg value of

nanotube is changed from 0.215 eV in pristine tube to 0.220 and 0.213 eV in the LA/CNT complexes, respectively. Since the conductivity is exponentially correlated with negative value of Eg, [59] it is expected that the adsorption of LA on CNT surface causes a significant change in its electrical conductivity.

In addition, the values of HOMO-LUMO gaps calculated using dispersion corrected version of DFT method (DFT-D/GGA) with those obtained based on DFT/GGA calculations were also compared in Table 2. A closer look at the Table 2 indicates that for the pristine CNTs with (4,4), (5,5), and (7,7) chiralities, DFT/GGA method predicts greater HOMO-LUMO gaps relative to the values calculated at DFT-D/GGA level. On the other hands, the results illustrated that for the modified CNTs in the gas phase, the calculated HOMO-LUMO gaps by DFT-D/GGA method for the CNT with (5,5), (6,6), and (7,7) chiralities are greater than values obtained by DFT/GGA method, showing the influence of the inclusion of vdW forces in the system.

The adsorption configurations of the lactic acid in two different modes can be qualitatively understood based on the electron distribution on the model CNTs. The HOMOs and LUMOs of pristine SWCNTs considered in present study and their complexes with lactic acid in two mentioned modes in the gas phase are plotted in Figure S1. In pristine SWCNTs, the HOMOs are delocalized uniformly on the nanotube sidewall and LUMOs are uniformly delocalized onto the alternate rings of carbon atoms in the nanotube sidewalls. This indicates that in armchair SWCNTs, the frontier orbital contribution from HOMO and LUMO are delocalized along nanotube sidewalls because of metallic armchair nanotubes are more polarizable compared to zigzag counterparts. On the other hands, after LA adsorption onto CNTs, no major alterations in the location of HOMO and LUMO orbitals are observed which point to this fact that the weak physisorption of LA does not modify the frontier orbital distribution of the SWCNTs and the

contribution to electronic state is basically from the SWCNTs. Moreover, a closer look at the Fig. S1 indicates LA molecule does not show significant contribution either toward the HOMO or LUMO. This trend in the observed frontier orbital distribution verifies that weakly adsorbed LA does not perturb the electronic levels of SWCNTs.

The calculated molecular electrostatic potential (MEP) on the molecular surfaces is illustrated in Figure S2. Generally, MEP on the molecular surface was calculated to find intermolecular properties such as the charge distribution, which showed the reactivity of the target aggregates. Figure S2 shows that the MEP changes for the charge distribution after a molecule is approaching to the carbon nanotubes. Generally, the negative electrostatic potential is related to the HOMO orbital and positive ones related to the LUMO orbitals. In addition, the isovalues shows regions that indicate the electronegativity and the partial charges on the different atoms of the molecule along with the total electron density. In the optimized geometries, the adsorption of the lactic acid molecule onto the pristine nanotube displays charge transfer between the oxygen atoms of LA and the nanotube surfaces at the adsorption sites which is due to an electrostatic interaction. In some case a strong coupling is observed that maybe responsible for structural alterations such as diameter change in CNTs.

3.4 Density of states

To further elucidate the electronic properties of the SWCNTs and modified SWCNTs, total electronic density of states (TDOS) and local DOS of CNTs (LDOS) are studied. Fig. 2 illustrates total density of state (TDOS) of free lactic acid and projected density of state (PDOS) of LA in (CNT+LA) system, respectively. The DOS and PDOS of all species are drawn in the −1

to 0.6 Hartree ranges, in order to show the electronic structures near the Fermi level. From Fig. 2, we found that the DOS of an isolated lactic acid have distinct peaks corresponding to separate energy levels, which belongs to an insulator, due to the extensive energy gap near the Fermi level. On the other hands, after adsorption of lactic acid on SWCNTs with different chirality, their PDOS demonstrates alteration and the peaks move to the low energy level near Fermi level of LA, and the energy gaps change narrower and as a result, the LA molecule becomes conductive.

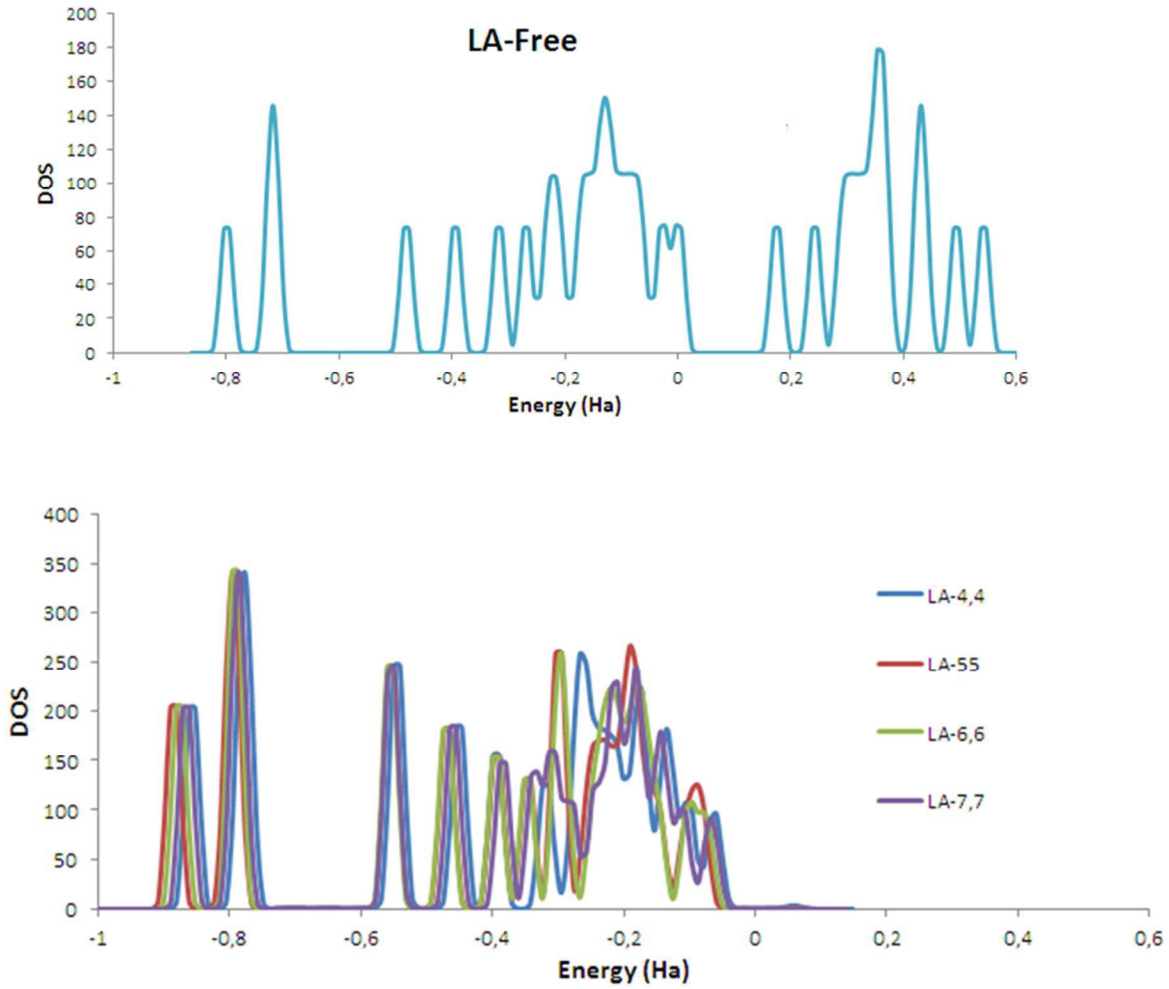

Fig. 2. The calculated total density of states (TDOS) of free lactic acid (top) and adsorbed lactic acid on SWCNTs in (CNT+LA) systems in the gas phase at DFT-D/GGA level of theory

The calculated density of states (DOS) for pure and modified SWCNTs with lactic acid in mode 1 and mode 2 are shown in Fig. 3a, 3b, and 3c, respectively. For the pristine CNTs the important peaks are appeared as follows. For the carbon nanotube with (4,4) chirality, the dominated peaks are observed at -0.68, -0.64, -0.53, -0.47, -0.38, -0.33, -0.31, -0.27, -0.16, -0.11 and -0.07 (Ha) which are below the Fermi level. Also, a peak at 0.06 Ha was observed above the Fermi level. For the SWCNT with (5,5) chirality important peaks below the Fermi level appeared at -0.68, -0.64, -0.54, -0.47, -0.41, -0.34, -0.31, -0.26, -0.23, -0.17 and -0.09 (Ha). On the other hands, with comparison to CNT with (5,5) chirality, the pristine CNTs with (6,6) and (7,7) chirality, corresponding important peaks slightly shifts to greater values. For example, two dominate peaks appeared at -0.27 and -0.23 Ha in CNT with (5,5) chirality, observed at -0.26 and -0.22 Ha for the CNT with (7,7) chirality. The results of calculated PDOSs of CNTs in complexes are presented in Fig. 3. The variations in the total DOS of CNTs in (CNT+LA) system show the interaction between the lactic acid molecule and carbon nanotube surface. The dominate peaks for the CNT with (4,4) chirality after adsorption of lactic acid through its carboxylic acid group (mode 1) appeared at -0.71, -0.66, -0.58, -0.51, -0.47, -0.39, -0.28, -0.16 (Ha) which are below the Fermi level, and in compare with pristine CNT, are shifted to negative values. Similar results observed for LA adsorption on CNT with (5,5) chirality where peaks shifted to -0.70, -0.65, -0.58, -0.53, -0.46, -0.41, -0.32, -0.26, -0.20, and -0.07 (Ha), respectively. On the other hands, adsorption of lactic acid through its hydroxyl group changed peaks in DOS diagram. For example, after adsorption of LA on CNT with (6,6) chirality, the important peaks shifted from -0.65, -0.61, -0.55, -0.54, -0.46, -0.42, -0.63, -0.25, -0.19, -0.14, -0.08, -0.04 (Ha) below the Fermi level to -0.66, -0.62, -0.57, -0.53, -0.46, -0.43, -0.36, -0.26, -0.19, and -0.07 (Ha), respectively. The results of DOS calculation also shows that non-covalent functionalization of

SWCNTs with lactic acid can give rise to new impurity states near -0.8 eV suggesting carbon nanotubes can act as selective sensors for LA molecule. As plotted in Fig. 3, the DOS of modified SWCNTs continuous at Fermi level, which suggests functionalized SWCNTs, are conductor.

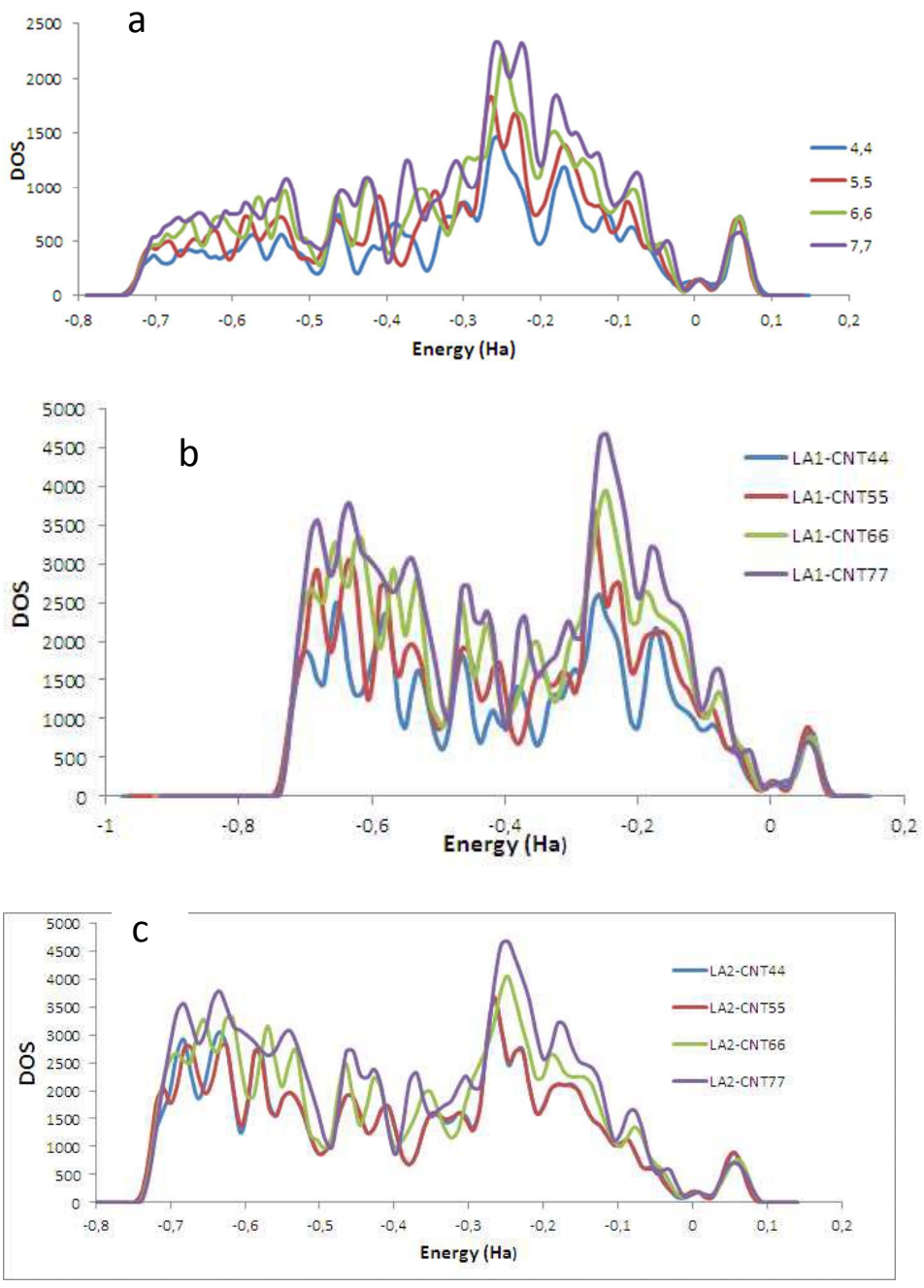

Fig. 3. The calculated total density of states (TDOS) of pristine carbon nanotubes (top), and projected density of state of modified CNTs in mode 1 (middle) and modified CNTs in mode 2 (below) in the (CNT+LA) system

The more detailed insight on the role of frontier orbitals in modulation of nanotube electronic properties and its contribution toward the DOS can be obtained with the analysis of PDOS. Since in SWCNTs the s and p orbitals are of major importance, the PDOS of them considered and plotted in Fig. 4. The trend in PDOS suggests that in the vicinity of Fermi region, only the 2p orbitals have contribution while s orbitals have insignificant contribution toward PDOS. Therefore and with respect to Fig. 2, it is evident that the orbital contribution towards PDOS is basically from the p-orbitals of SWCNTs in the vicinity of Fermi level with LA having negligible contribution.

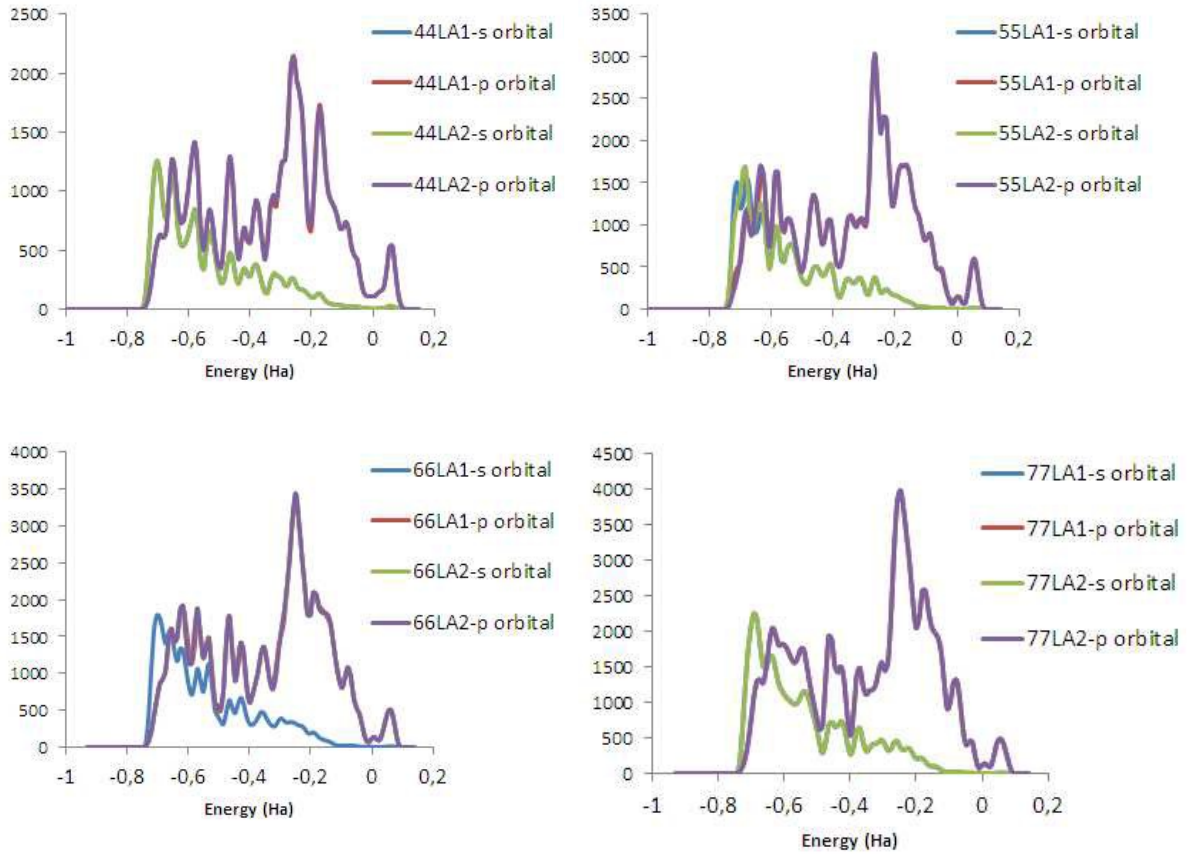

Fig. 4. The calculated projected density of states (PDOS) of aggregates of SWCNTs and LA in the gas phase at DFT-D/GGA level of theory

3.5 Global reactivity descriptors

The global indices of reactivity for the adsorption of LA on SWCNTs in the gas phase and water as the solvent are presented in Table 4. The results in Table 4 indicate the global hardness (η) values of pristine CNTs in some cases vary after modification with LA. For example, with approaching of LA through its carboxylic acid and hydroxyl groups to pristine (4,4) SWCNT, the η value increased from 0.234 to 0.238 and 0.236 eV, respectively. Therefore, one can conclude that modification of CNT with (4,4) chirality, decrease its reactivity. In the other hands, while approaching of lactic acid via its carboxylic group exhibits a drastic increasing of η value (0.002 eV), interaction through its hydroxyl group decrease the hardness value (0.001 eV) compared with pristine nanotube counterpart. On the other hands, one can study the size effect of CNTs on their reactivity after adsorption of lactic acid. With respect to the adsorption through its carboxylic group (mode 1), the global hardness for the CNTs with (4,4) and (5,5) chiralities increased but for larger rings remained unchanged.

The μ parameter shows the escaping tendency of electrons from a molecular system in its equilibrium state. The greater the μ value less stable or more reactive is the species. The calculated μ values for the pristine and modified SWCNTs indicates after functionalization of CNT with (4,4) chirality with LA by approaching through its carboxylic or hydroxyl groups, the chemical potential increased from -3.614 to -3.893 and -3.949 eV, respectively. Similar behavior

observed for the CNT with (5,5) chirality, where μ value after adsorption of lactic acid increased from -3.668 to -3.721 eV. In addition, adsorption of LA on CNT with (6,6) chirality caused reactivity of nanotube increased from -3.684 to -3.871 eV. In overall, it is concluded that adsorption of LA through both hydroxyl or carboxylic groups increase chemical potential of nanotubes. Interestingly, when complexes studied in water as the solvent variation of chemical potential changed.

Table 4
Calculated global reactivity descriptors (eV) for the pristine and modified SWCNTs in the gas phase at DFT-D/GGA level of theory

System	Gas phase			Solvent phase		
	μ	η	ω	μ	η	ω
(4,4)	-3,614	0,234	27,960	-3,967	0,229	34,360
(4,4)CNT-LA1	-3,893	0,238	31,839	-3,978	0,229	34,551
(4,4)CNT-LA2	-3,949	0,236	33,039	-3,992	0,228	35,016
(5,5)	-3,668	0,108	62,561	-4,014	0,113	71,592
(5,5)CNT-LA1	-3,721	0,110	62,936	-4,032	0,114	71,303
(5,5)CNT-LA2	-3,636	0,107	62,051	-3,995	0,112	71,552
(6,6)	-3,684	0,162	41,888	-4,039	0,165	49,435
(6,6)CNT-LA1	-3,871	0,162	46,380	-4,057	0,167	49,279
(6,6)CNT-LA2	-3,942	0,161	48,259	-4,024	0,165	49,068
(7,7)	-3,703	0,196	34,980	-4,057	0,200	41,241
(7,7)CNT-LA1	-3,738	0,196	35,645	-4,068	0,201	41,258
(7,7)CNT-LA2	-3,698	0,195	35,145	-4,049	0,198	41,400

While LA adsorption through carboxylic and hydroxyl groups on CNT with (4,4) chirality slightly increased its μ value, for other CNTs only adsorption via carboxylic acid (mode 1) increased the reactivity and approaching through hydroxyl group decreased their reactivities. The electrophilicity index (ω) proposed as a measure of energy lowering due to maximal electron flow between donor and acceptor. [60] As it can be seen from Table 4, the ω value increases with functionalization, which illustrates the increase in electrophilic character or electrophilicity of

modified CNTs. We investigated the effect of solvent on global reactivity descriptors. The results of calculated global reactivity descriptors illustrated in Table 4 show while with going from the gas phase to water, chemical hardness of pristine and modified CNTs with (4,4) chirality decreased, this parameter for the CNTs with (5,5), (6,6), and (7,7) chiralities increased. Moreover, the results indicate with going from the gas phase to the solvent the electrophilicity of CNTs and modified CNTs increased.

4. Conclusion

The structure and electronic properties of non-covalent functionalization of SWCNTs with LA was studied using the dispersion corrected hybrid DFT method. Two different paths were selected for approaching of LA to outer surface of CNTs: through its hydroxyl and carboxylic acid groups. The calculations showed that the adsorption of LA onto outer wall of CNTs is energetically favorable. The most effective interaction observed for the adsorption of LA on the surface of SWCNT with (4,4) chirality. The adsorption process changed the geometrical parameters of CNTs especially the diameters was investigated. The effect of solvent (water) was also studied using COSMO model. Our results indicated that both geometrical parameters and adsorption energies affected by solvent. The electronic properties such as HOMO-LUMO energy gap, MEP, TDOS, and PDOS parameters analyzed. It was concluded that the E_g energy values altered after adsorption of LA on pristine SWCNTs. However, the distribution of orbitals did not changed significantly by LA loading on CNTs. In addition, adsorption process slightly changed the DOSs of carbon nanotubes. Global reactivity descriptors calculated in the gas phase and water as the solvent. Interestingly, the parameters affected by water, but a regular change did not observed.

Acknowledgement

We would like to thank Isfahan University of Technology (IUT) for the financial support (Research Council Grant).

References

1. J. N. Coleman, U. Khan, W. J. Blau and Y. K. Gun'ko, *Carbon*, 2006, **44**, 1624–1652.
2. M. B. Bryning, M. F. Islam, J. M. Kikkawa and A. G. Yodh, *Adv. Mater.*, 2005, **17**, 1186–1191.
3. K. Wang, P. Zhao, X. M. Zhou, H. P. Wu and Z. X. Wei*, J. Mater. Chem.*, 2011, **21**, 16373–16378.
4. Z. P. Li, Y. J. Mi, X. H. Liu, S. Liu, S. R. Yang and J. Q. Wang, *J. Mater. Chem.*, 2011, **21**, 14706–14711.
5. H. Cao, S. Liu, W. Tu, J. Bao and Z. Dai, *Chem. Commun.*, 2014, **50**, 13315-13318
6. C. Oelsner, M. A. Herrero, C. Ehli, M. Prato and D. M. Guldi, *J. Am. Chem. Soc.*, 2011, **133**, 18696-18706
7. R. Marches, P. Chakravarty, I. H. Musselman, P. Bajaj, R. N. Azad, P. Pantano, R. K. Draper and E. S. Vitetta*, Int. J. Cancer,* 2009, **125**, 2970-2977
8. R.J. Brodd. *Chem. Rev.*, 2003; **104**, 4245–4269
9. A.I. Oliva-Aviles, F. Aviles and V. Sosa, *Carbon* 2011, **49**, 2989 – 2997
10. C.-K. Huang, Y. Ou, Y. Bie, Q. Zhao and. D. Yu, *Appl. Phys. Lett.* 2011, **98**, 263104 (4pp)
11. P. Liu, Y. Wei, K. Liu, L. Liu, K. Jiang, and S. Fan, *Nano Lett*., 2012, **12**, 2391–2396
12. S. Choudhary and S. Qureshi, *Phys. Lett. A* 2011, **375**, 3382-3385

13. N. Chandra, S. Nimilae and C. Shet, *Phys. Rev. B* 2004, **69**, 94101–94111

14. L. Ding, Z. Zhang, T. Pei, S. Liang, S. Wang, W. Zhou, J. Liu and L.-M. Peng, *ACS Nano*, 2012, **6**, 4013–4019

15. A.O. Monteiro, P.B. Cachim and P.M.F.J. Costa, *Diamond Relat. Mater.* 2014, **44,** 11–25

16. M.-F. Yu, O. Lourie, M. J. Dyer, K. Moloni, T. F. Kelly and R. S. Ruoff, *Science,* 2000, **287**, 637–640.

17. V. Ivanovskaya, C. Köhler and G. Seifert, *Phys. Rev. B* 2007, **75**, 075410-7

18. D. Jana a, C.-L. Sun, L.-C. Chen and K.-H. Chen, *Prog. Mater Sci.* 2013, **58**, 565–635

19. R. B. Sharma, D. J. Late, D. S. Joag, A. Govindaraj and C. N. R. Rao *Chem Phys Lett* 2006, **428**, 102–108

20. A. Kaczmarek, T. C. Dinadayalane, J. Łukaszewicz and J. Leszczynski *Int. J. Quantum. Chem.* 2007, **107**, 2211–2219

21. T. C. Dinadayalane, A. Kaczmarek, J. Łukaszewicz and J. Leszczynski *J. Phys. Chem. C.* 2007, **111**, 7376–7383

22. S. S. Wu, Q. B. Wen, W. T. Zheng and Q. Jiang *Nanotechnolgy* 2007, **18**, 165702. (7pp).

23. M. F. Mora, C. E. Giacomelli and C. D. Garcia, *Anal. Chem.*, 2009, **81**, 1016–1022.

24. J. McCarroll, H. Baigude, C.-S. Yang and T. M. Rana, *Bioconjugate Chem.*, 2009, **21**, 56–63.

25. Q. Lu, J. M. Moore, G. Huang, A. S. Mount, A. M. Rao, L. L. Larcom and P. C. Ke, *Nano Lett.*, 2004, **4**, 2473–2477.

26. J. T. Robinson, K. Welsher, S. M. Tabakman, S. P. Sherlock, H. Wang, R. Luong and H. Dai, *Nano Res.,* 2010, **3**, 779–793

27. A. Narladkar, E. Balnois, and Y. Grohens, *Macromol. Symp.* 2006, **241**, 34-44

28. M. Kleerebezem and J. Hugenholtz, *Curr. Opin. Biotechnol.* 2003, **14**, 232-237

29. W. H. Munyon and D.J. Merchant *Exp. Cell Res.* 1959, **17**, 490–498

30. W. Amass, A. Amass and B. Tighe, *Polymer International* 1998, **47**, 89–144

31. R. Datta, S.P. Tsai, P. Bonsignore, S.H. Moon, J.R. Frank and *FEMS Microbiol. Rev*. 1995, **16**, 221–231

32. P. Maki-Arvela, Irina L. Simakova, T. Salmi and D.Y. Murzin, *Chem. Rev.* 2014, **114**, 1909-1971

33. B.P. van Eijck *J. Mol. Spectrosc.* 1983, **101**, 133-138.

34. A. Borba, A. Gomez-Zavaglia, Leszek Lapinskic and R. Fausto, *Phys . Chem. Chem. Phys.*, 2004 , **6** , 2101– 108

35. A. Shouten, J. Kanters and J. van Krieken, *J. Mol. Struct.,* 1994, **323**, 165-168.

36. G. Cammas, M. Morssli, E. Fabregue and L. Bardet, J. Raman Spectrosc. 1991, **22**, 409-413,

37. F. Berruyer-Penaud, G. Bouchoux, O. Payen and M. Sablie, *J. Mass Spectrom.* 2004; **39**, 613–620

38. M. Pecul, A. Rizzo and J. Leszczynski, *J. Phys. Chem. A*, 2002, **106**, 11008-11016.

39. A. Smaga and J. Sadlej, *J. Phys. Chem. A* 2010, **114**, 4427–4436

40. A. N. Chermahini, A. Teimouri and H. Farrokhpour, *Appl. Surf. Sci.* 2014, **320**, 231-236

41. H. Hafizi, A. N. Chermahini, G. Mohammadnezhad and A. Teimouri, *Appl. Surf. Sci.* 2015, **329**, 87-93

42. B. Delley, *J. Chem. Phys.* 1990, **92**, 508–517.

43. B. Delley, *J. Chem. Phys.* 2000, **113**, 7756–7764

44. J.P. Perdew and Y. Wang, *Phys. Rev. B* 1992, **45**, 13244–13249.

45. T. Liang, W. X. Li and H. Zhang *J. Mol. Struct. (THEOCHEM)* 2009, **905**, 44-47

46. F. Ortmann, F. Bechstedt and W. G. Schmidt, *Phys. Rev. B* 2006, **73,** 205101-205110

47. B. Delley, *Mol. Simul.* 2006, **32**, 117–123

48. J. Tomasi and M. Persico, *Chem. Rev.* 1994, **94**, 2027–2094

49. . A. C. Kolmel and A. Klamt, *J. Chem. Phys.* 1995, **103,** 9312–9321.

50. A. Klamt J. Phys. Chem., 1995, 99, 2224–2235

51. M. Anafcheh and R. Ghafouri, Superlattice Microst. 2013, 60, 1-9.

52. B.G. Kim, X.X. Li, and P. Blowers, *Langmuir* 2009, **25,** 2781–2789

53. N.A. Benedek, I.K. Snook, K. Latham, and I. Yarovsky, *J. Chem. Phys.* 2005, **122** 144102-8

54. Y. Inada and H. Orita, *J. Comput. Chem.* 2008, **29**, 225-232.

55. P. J. Thornalley *Biochem. J.* 1990, **269**, 1–11

56. M. M. F. Choi *Food Chem.* 2005, **92**, 575-581

57. W. Trettnak and O. S. Wolfbeis, *Anal. Lett.* 1989, **22**, 2191-2197

58. Y. Zhao, X. Wu, J. Yang and X. C. Zeng, *Phys. Chem. Chem. Phys.* 2011, 13, 11766-11772.

59. N. Saikia and R. C. Deka, *Int. J. Quantum. Chem.* 2012, **113**, 1272-1284

60. R.G. Parr, L.V. Szentpaly, and S.B. Liu, *Electrophilicity index, J. Am. Chem. Soc.* 1999, **121**, 1922–1924.